

## High-Efficiency InP IMPATT Diodes for High-Frequency Power Generation<sup>†</sup>

Chien-Chung Chen, Richard K. Mains, George I. Haddad and Heribert Eisele

*Department of EECS, The University of Michigan, Ann Arbor, Michigan 48109-2122*

### Abstract

Numerical simulation based on the average-energy transport model shows that InP IMPATT diodes in general have higher DC-to-RF conversion efficiency and higher negative resistance than GaAs diodes at high frequencies, which implies that InP is a better material than GaAs for building two-terminal transit-time devices. Reasons for the superiority of InP diodes over GaAs diodes are:

- InP has higher drift velocities than GaAs.
- The decrease of electron velocity at increased electric field is faster in InP. When the space-charge effect is strong, electrons are more localized in InP diodes.
- InP diodes are much more IMPATT-like (i.e. tunneling is less significant) than GaAs ones and therefore have higher efficiency.
- The impact ionization of InP is smaller than GaAs at low electric fields while higher at high fields. Because of this, the generated charge pulse is sharper in InP diodes, which also leads to higher efficiency.
- InP has better thermal conductivity than GaAs.

Simulation results for InP diodes intended for power generation for W-band and above are presented in this paper. Comparison of RF performance with GaAs diodes are also presented.

---

<sup>†</sup>This work was supported by NASA under contract NAGW-1334.

## 1 Introduction

Since the proposal by Read[1] in 1958 and the first report of experimental observation of RF oscillations from a Si diode by Johnston *et al.* in 1965[2], IMPATT diodes have been extensively studied and used as high-power and high-efficiency solid-state microwave power sources. GaAs IMPATT diodes, due to negative differential electron mobility of GaAs, usually achieve higher DC-to-RF conversion efficiency than Si diodes at low frequencies, e.g. 35.5% at 8.15 GHz from a GaAs diode reported by Kim and Matthei[3] vs. 11.8% at 8.5 GHz from a Si diode reported by Seidel and coworkers[4]. At high frequencies such as 94 GHz, the interband tunneling current severely degrades the conversion efficiency of the hi-lo structure, while in the flat-doped structure the positive differential electron mobility of Si is preferred to the negative differential electron mobility of GaAs. Therefore, GaAs diodes do not have significant advantage over Si diodes at high frequencies.

According to the InP impact ionization rates measured at various temperatures by Taguchi *et al.*[5], InP has higher impact ionization rates at high electric fields but lower impact ionization rates at low electric fields than GaAs. The interband tunneling rate calculation based on Kane's theory[6] indicates that, although the interband tunneling generation rates of InP are higher than those of GaAs, the difference is not as significant as that for impact ionization generation rates. It is therefore expected that the tunneling current is smaller in an InP diode than in a GaAs diode. Other advantages of InP are higher electron saturation velocity, higher thermal conductivity and higher differential electron mobility. For these reasons, InP diodes have the potential of achieving better RF performance than GaAs diodes at high frequencies.

This paper presents the numerical simulation model, material parameters and simulation results of GaAs and InP diodes. Simulation results for GaAs and InP diodes will be compared to show the superiority of InP diodes over GaAs ones.

## 2 Simulation Model and Material Parameters

The simulation programs in addition to Poisson's equation solve the following equations to obtain the diode states:

$$J_p = qp\mu_p(E)E - \frac{\partial [qD_p(E)p]}{\partial x} \quad (1)$$

$$J_{n1} = qn_1\mu_{n1}(w_1)E + \frac{\partial [qD_{n1}(w_1)n_1]}{\partial x} \quad (2)$$

$$J_{n2} = qn_2\mu_{n2}(w_2)E + \frac{\partial [qD_{n2}(w_2)n_2]}{\partial x} \quad (3)$$

$$\frac{\partial w_1}{\partial t} = \frac{J_{n1}}{qn_1} \frac{\partial w_1}{\partial x} + \frac{J_{n1}E}{n_1} - \frac{w_1 - w_{th}}{\tau_{w1}(w_1)} \quad (4)$$

$$\frac{\partial w_2}{\partial t} = \frac{J_{n2}}{qn_2} \frac{\partial w_2}{\partial x} + \frac{J_{n2}E}{n_2} - \frac{w_2 - w_{th}}{\tau_{w2}(w_2)} \quad (5)$$

$$\frac{\partial p}{\partial t} = -\frac{1}{q} \frac{\partial J_p}{\partial x} + G_p \quad (6)$$

$$\frac{\partial n_1}{\partial t} = \frac{1}{q} \frac{\partial J_{n1}}{\partial x} + G_{n1} \quad (7)$$

$$\frac{\partial n_2}{\partial t} = \frac{1}{q} \frac{\partial J_{n2}}{\partial x} + G_{n2} \quad (8)$$

where  $w_{th} = \frac{3}{2}k_B T$  is the thermal equilibrium energy for electrons, and the carrier generation rates  $G_p$ ,  $G_{n1}$  and  $G_{n2}$  are given by

$$G_p = G_{II} + G_T + G_{th} - R_{th} \quad (9)$$

$$G_{n1} = G_{II} + G_T + G_{th} - R_{th} + \frac{n_2}{\tau_{n2-1}(w_2)} - \frac{n_1}{\tau_{n1-2}(w_1)} \quad (10)$$

$$G_{n2} = \frac{n_1}{\tau_{n1-2}(w_1)} - \frac{n_2}{\tau_{n2-1}(w_2)} \quad (11)$$

In the simulation programs, holes follow the drift-diffusion equation, while electrons are described by a variation of the two-valley drift-diffusion equation with the mobilities and diffusion coefficients being functions of electron energies instead of the electric field. The electron energies are governed by the two energy equations.

Close examination of the above equations reveals that the momentum relaxation times for electrons are actually neglected in the program. This is justified as long as the momentum relaxation times are much smaller than the period of the RF voltage.

The materials used for devices in this work are GaAs and InP. Since these devices are intended for RF power generation, the material lattice temperature is usually very high. 500°K is assumed throughout this work. The majority of the material parameters used by the simulation programs are generated by a Monte Carlo (MC) program. This MC program provides the values of electron velocities, diffusion coefficients, relaxation times and electron energies as functions of the electric field up to 3000 kV/cm. The methods used to evaluate the relaxation times are similar to those proposed by Stewart *et al.*[7], while the electron (longitudinal) diffusion coefficients are calculated in the MC program using the method mentioned by Fawcett[8]. Other electron parameters such as the material intrinsic concentration and electron-hole recombination lifetime and all the hole parameters are set according to empirical expressions or assumed values.

Two important material parameters used by the simulation programs are the impact ionization and tunneling rates. They have very profound effects on the device operation, but still lack adequate determination in the electric field range where the devices are operated (up to 3000 kV/cm). The impact ionization generation rate is expressed as

$$G_{II} = (\alpha_n J_n + \alpha_p J_p)/q \quad (12)$$

For GaAs,  $\alpha_n$  and  $\alpha_p$  are given by

$$\alpha_n = A_n \exp \left[ -(B_n/E)^2 \right] \quad (13)$$

$$\alpha_p = A_p \exp \left[ -(B_p/E)^2 \right] \quad (14)$$

with the following values being used for GaAs at 500°K

$$A_n = A_p = 2.1205 \times 10^5 \text{ cm}^{-1}$$

$$B_n = B_p = 6.71 \times 10^5 \text{ V/cm}$$

For  $\alpha_n$  and  $\alpha_p$  in InP, we adopt the expressions given by Okuto and Crowell[9] as follows

$$\alpha_n, \alpha_p = \frac{qE}{E_{th}} \exp \left( 0.217 (E_{th}/E_R)^{1.14} - \left\{ \left[ 0.217 (E_{th}/E_R)^{1.14} \right]^2 + \left( \frac{E_{th}}{qE\lambda} \right)^2 \right\}^{1/2} \right) \quad (15)$$

with the parameters  $E_{th}$ ,  $E_R$  and  $\lambda$  fitted by Taguchi *et. al.*[5], which leads to

$$\alpha_n = \frac{E}{1.78} \exp \left\{ 31.75 - \left[ 31.75^2 + \left( \frac{8.75 \cdot 10^6}{E} \right)^2 \right]^{1/2} \right\}$$

$$\alpha_p = \frac{E}{1.59} \exp \left\{ 47.0 - \left[ 47.0^2 + \left( \frac{9.75 \cdot 10^6}{E} \right)^2 \right]^{1/2} \right\}$$

for InP at 500°K, where the unit of electric field  $E$  is V/cm, and the unit of  $\alpha_n$  and  $\alpha_p$  is 1/cm.

As to the interband tunneling rate, we adopt the expression which complies with the highly idealized form proposed by Kane[6] as shown below

$$G_T = A_T E^2 \exp(-B_T/E) \quad (16)$$

For GaAs at 500°K, we use

$$A_T = 1 \times 10^{20} \text{ cm}^{-1}\text{s}^{-1}\text{V}^{-2}$$

$$B_T = 1.2 \times 10^7 \text{ V/cm}$$

And for InP at 500°K

$$A_T = 1.37 \times 10^{20} \text{ cm}^{-1}\text{s}^{-1}\text{V}^{-2}$$

$$B_T = 1.178 \times 10^7 \text{ V/cm}$$

The dead space for impact ionization and interband tunneling is considered in the simulation program. For impact ionization, the energy relaxation effect automatically includes the dead space in the model. As to interband tunneling, we use the bandgap to determine the dead space as illustrated in Figure 1. The principle is that tunneling only occurs where there are empty states in the conduction band and filled states in the valance band.

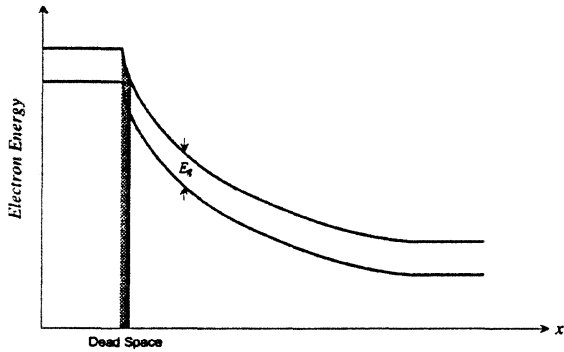


Figure 1: Dead space for interband tunneling.

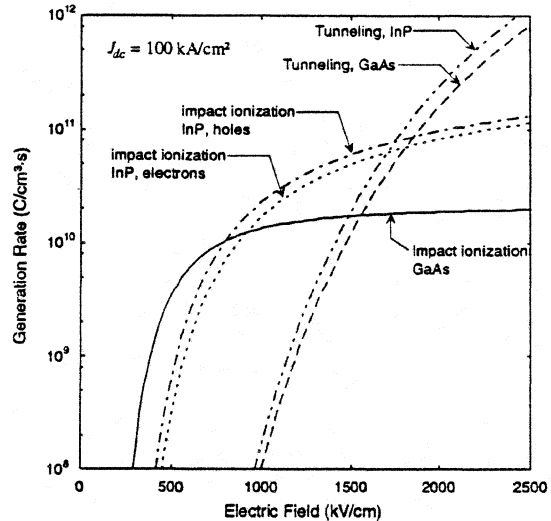


Figure 2: The impact ionization and tunneling generation rates for GaAs and InP at 500°K.

In the simulation programs, all material parameters for electrons except the tunneling rate are tabulated according to the electron energy. In other words, they are treated as functions of the electron energy instead of the electric field. The tunneling rate is considered as a function of the electric field since it is related more to the electric field that electrons in the valence band experience than to the energy of electrons in the conduction band. Figure 2 shows the impact ionization and tunneling generation rates for 500°K GaAs that are used in the simulation programs. Inside the simulation program, the impact ionization rate is transformed into a function of electron energy.

The metal-semiconductor contact resistances are estimated by solving the Schrödinger's equation. The p-type Ohmic contact resistance for InP is very high due to the high barrier height for holes. This high p-type contact resistance can be greatly reduced by using lattice-matched InGaAs cap layers or Schottky collectors[10]. Thermal resistance of a diode is calculated using the approximate thermal model discussed in [11]. Devices with high thermal resistance should be biased at low current densities or operate in the pulsed mode in order to keep the p-n junction temperature below 500°K.

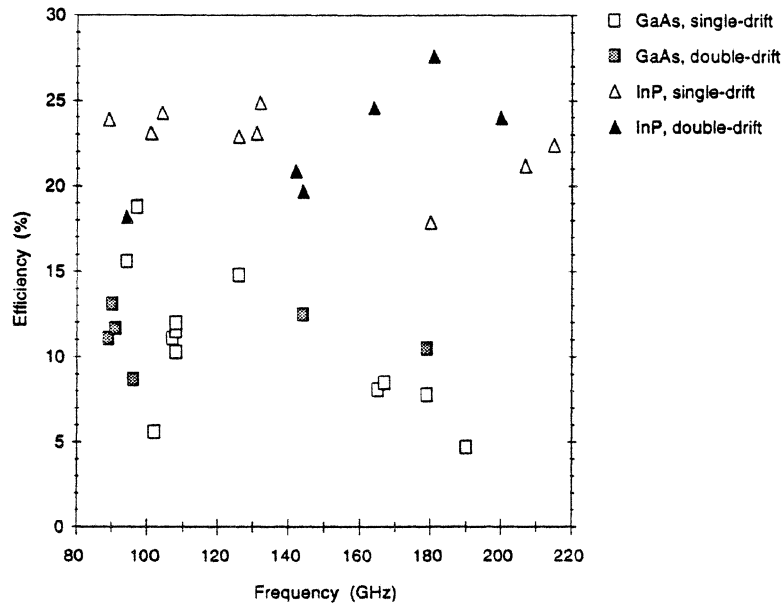


Figure 3: The efficiency for GaAs and InP diodes at various frequencies.

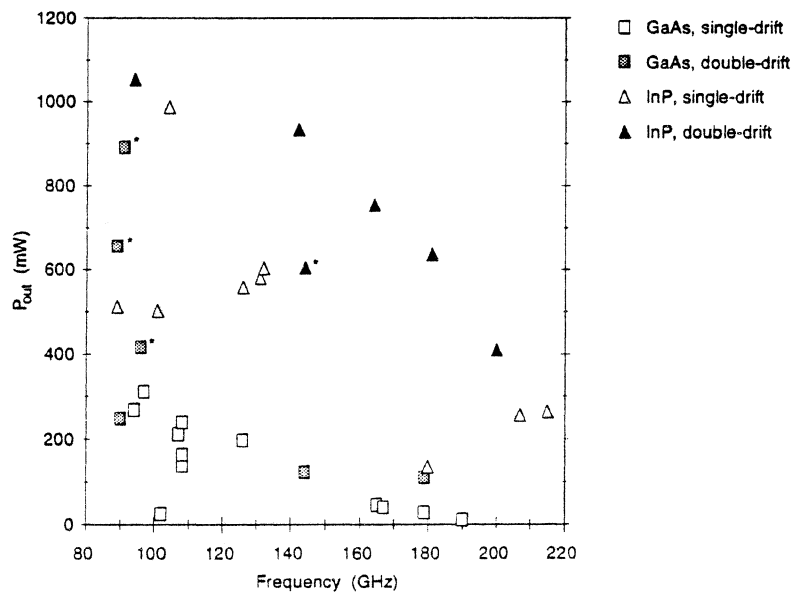


Figure 4: The 1-Ω RF output power for GaAs and InP diodes at various frequencies. Points marked with \* represent average power from pulsed diodes.

### 3 Simulation Results and Discussion

Sixteen GaAs diodes and sixteen InP diodes designed to operate at 94 GHz and above were simulated in this work. Figures 3 and 4 present the DC-to-RF conversion efficiency  $\eta$  and 1- $\Omega$  RF output power  $P_{1\Omega}$  calculated for all the structures simulated in this work. It can be clearly seen that InP diodes have significantly higher conversion efficiency than GaAs diodes. Part of the reason why InP diodes have higher conversion efficiency can be explained by Figure 5, which displays typical injected and induced current waveforms of GaAs and InP diodes obtained from simulation. First, the carrier injection angle in the InP diode is larger than that in the GaAs diode, indicating lower contribution of interband tunneling to the generation current in the InP diode. Second, the InP diode has sharper turn-on and turn-off characteristics in the injected current due to the steeper slopes of the impact ionization generation rates in InP shown in Figure 2. The higher breakdown field of InP shown in Figure 2 allows higher electric field in the drift region, which also leads to a higher conversion efficiency. Third, higher induced current peak near  $270^\circ$  in the InP diode, which results from electrons' high-speed surfing through the drift region at low fields. Fourth, the higher negative electron differential mobility in InP causes the electron pulse to get sharper as it travels through the drift region. Less electrons are left in the drift region at the end of an RF cycle, resulting in a lower induced current in the first half of the next RF cycle.

As the simulation results indicate, the device negative resistance, in many occasions, is more important than the conversion efficiency since the matching condition requires a diode with low negative resistance to have small cross-sectional area, while the negative resistance of a device is proportional to its RF output power. The double-drift structures have longer device lengths and therefore lower capacitance effects than the single-drift structures, making the RF output power of the double-drift diode significantly higher than that of the single-drift one. The higher carrier drift velocity of InP also leads to higher negative resistances of InP diodes, which explains the reason why InP diodes have much higher RF output power than GaAs ones as shown in Figure 4.



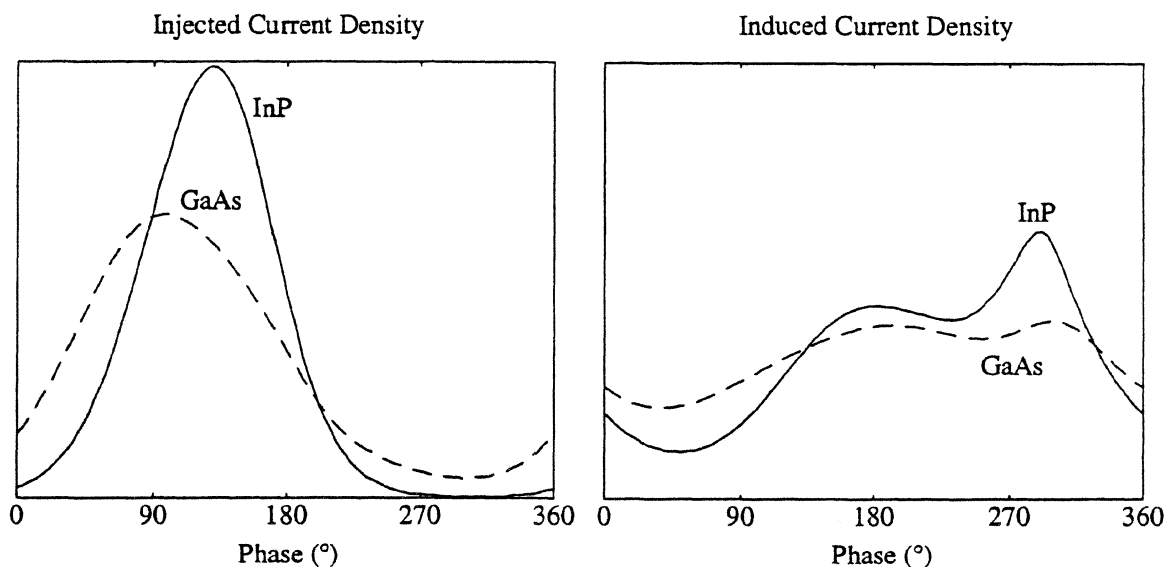


Figure 5: Typical injected and induced currents of the GaAs and InP diodes at high frequencies.

Devices having Schottky contacts in place of Ohmic contacts suffer less from the parasitic contact resistance, and therefore have higher conversion efficiency and overall negative resistance. Besides, the absence of the buffer layer required by the conventional Ohmic-contacted diode makes the thermal resistance of the Schottky-contacted diode much smaller.

Note that since the thermal conductivity of InP is about 25% higher than that of GaAs, InP diodes can be biased at higher current densities to achieve higher negative resistance and higher RF output power.

## 4 Conclusion

Numerical programs capable of simulating high-frequency transit-time diodes have been developed, for which the transport model and material parameters have been briefly discussed. Several GaAs and InP diodes are simulated. InP diodes, due to higher carrier drift velocities, higher thermal conductivity, higher negative differential electron mobility and higher impact ionization rates,

have better RF performance than GaAs.

## References

- [1] W. J. Read, "A Proposed High Frequency Negative Resistance Diode," *Bell System Tech. J.*, **33**, pp. 401–446, March 1958.
- [2] R. L. Johnston, B. C. DeLoach, Jr. and B. G. Cohen, "A Silicon Diode Oscillator," *Bell System Tech. J.*, **44**, pp. 369–372, February 1965.
- [3] C. K. Kim and W. G. Matthei, "GaAs Read IMPATT Diode Oscillators," *Proc. Fourth Biennial Electrical Engineering Conf.*, Ithaca, NY, pp. 299–305, August 1973.
- [4] T. E. Seidel, W. C. Niehaus and D. E. Iglesias, "Double-Drift Silicon IMPATT's at X-band," *IEEE Trans. Electron Dev.*, **ED-21**, pp. 523–531, August 1974.
- [5] K. Taguchi, T. Torikai, Y. Sugimoto, K. Makita and H. Ishihara, "Temperature Dependence of Impact Ionization Coefficients in InP," *J. Appl. Phys.*, **59**, January 1986.
- [6] E. O. Kane, "Theory of Tunneling," *J. Appl. Phys.*, **32**, pp. 83–91, 1961.
- [7] R. A. Stewart, L. Ye and J. N. Churchill, "Improved Relaxation-Time Formulation of Collision Terms for Two-Band Hydrodynamic Models," *Solid-State Electronics*, **32**, No. 6, pp. 497–502, 1989.
- [8] W. Fawcett, "Non-ohmic transport in semiconductors," *Electrons in Crystalline Solids*, International Atomic Energy Agency, Vienna, pp. 531–618, 1973.
- [9] Y. Okuto and C. R. Crowell, "Energy-Conservation Considerations in the Characterization of Impact Ionization in Semiconductors," *Phys. Rev. B*, **6**, pp. 3076–3081, 1972.

- [10] C.-C. Chen, "Non-Equilibrium Modeling of Mixed Tunneling and Avalanche Breakdown Effects in Transit-Time Diodes," Ph.D. Dissertation, 1994, The University of Michigan, Ann Arbor.
- [11] R. K. Mains and G. I. Haddad, "Properties and Capabilities of Millimeter-Wave IMPATT Diodes," *Infrared and Millimeter Waves*, **10**, pp. 111-231, 1983.